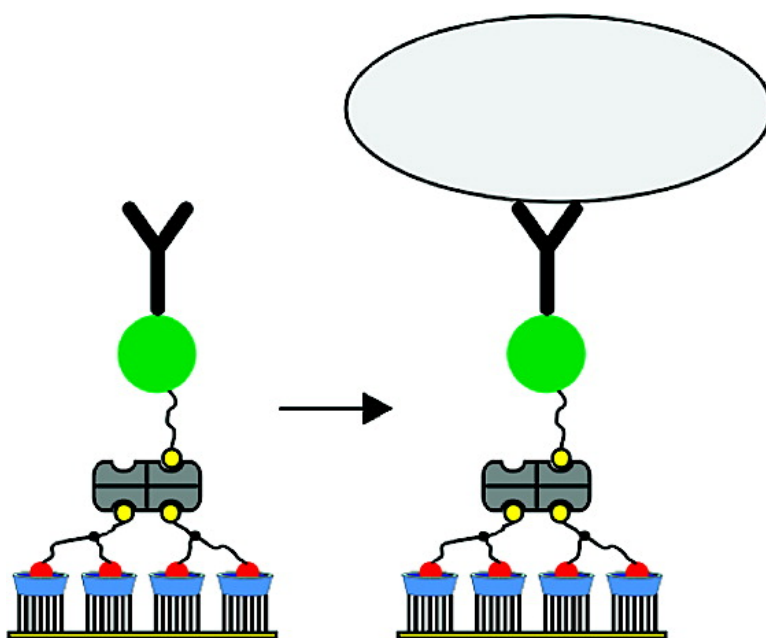


## Assembly of Bionanostructures onto #-Cyclodextrin Molecular Printboards for Antibody Recognition and Lymphocyte Cell Counting

Manon J. W. Ludden, Xiao Li, Jan Greve, Aart van Amerongen, Maryana Escalante, Vinod Subramaniam, David N. Reinhoudt, and Jurriaan Huskens

*J. Am. Chem. Soc.*, **2008**, 130 (22), 6964-6973 • DOI: 10.1021/ja078109v • Publication Date (Web): 08 May 2008

Downloaded from <http://pubs.acs.org> on February 8, 2009



### More About This Article

Additional resources and features associated with this article are available within the HTML version:

- Supporting Information
- Access to high resolution figures
- Links to articles and content related to this article
- Copyright permission to reproduce figures and/or text from this article

[View the Full Text HTML](#)

## Assembly of Bionanostructures onto $\beta$ -Cyclodextrin Molecular Printboards for Antibody Recognition and Lymphocyte Cell Counting

Manon J. W. Ludden,<sup>†</sup> Xiao Li,<sup>‡</sup> Jan Greve,<sup>‡</sup> Aart van Amerongen,<sup>\*,§</sup>  
Maryana Escalante,<sup>‡</sup> Vinod Subramaniam,<sup>‡</sup> David N. Reinhoudt,<sup>†</sup> and  
Jurriaan Huskens<sup>\*,†</sup>

*Molecular Nanofabrication Group and Laboratory of Biophysical Engineering, MESA<sup>+</sup> Institute for Nanotechnology and Institute for Biomedical Technology, University of Twente, P.O. Box 217, 7500 AE Enschede, The Netherlands, and Agrotechnology & Food Innovations, Wageningen University, Wageningen, The Netherlands*

Received October 25, 2007; E-mail: j.huskens@utwente.nl; aart.vanamerongen@wur.nl

**Abstract:** The assembly of complex bionanostructures onto  $\beta$ -cyclodextrin ( $\beta$ CD) monolayers has been investigated with the aims of antibody recognition and cell adhesion. The formation of these assemblies relies on host–guest, protein–ligand, and protein–protein interactions. The buildup of a structure consisting of a divalent bis(adamantyl)-biotin linker, streptavidin (SAV), biotinylated protein A (bt-PA), and an Fc fragment of a human immunoglobulin G (IgG-Fc) was studied with surface plasmon resonance (SPR) spectroscopy. Patterns of this bionanostructure were obtained via microcontact printing of the divalent linker at the molecular printboard, followed by the subsequent attachment of the proteins. Fluorescence microscopy showed that the buildup of these bionanostructures on the  $\beta$ CD monolayers is highly specific. On the basis of these results, bionanostructures were made in which whole antibodies (ABs) were used instead of the IgG-Fc. These ABs were bound to the SAV layer via biotinylated protein G (bt-PG) or via a biotinylated AB. These constructions yielded specifically bound ABs with a less than maximal density, as shown by SPR spectroscopy and atomic force microscopy (AFM). Finally, the immobilization of ABs to the molecular printboard was used to create platforms for lymphocyte cell count purposes. Monoclonal ABs (MABs) were attached to the SAV layer using bt-PG, an engineered biotin functionality, or through nonspecific adsorption. The binding specificity of the immobilized cells was the highest on the buildup made from bt-PG, which is attributed to an optimized orientation of the antibodies. An approximately linear relationship between the numbers of seeded cells and counted cells was demonstrated, rendering the platform potentially suitable for lymphocyte cell counting.

### Introduction

There has been considerable interest in the assembly of protein bionanostructures at surfaces for biosensing purposes. Examples of such complex bionanostructures at surfaces are, for example, the human chorionic gonadotropin (hGC) sensor reported by Knoll et al.,<sup>1</sup> and the sensor types described in a review by Wilchek, all based on the immobilization of antibodies at surfaces.<sup>2</sup> For many of these purposes, one needs control over adsorption strength and reversibility, protein orientation, and retention of biological function. Such requirements can only be met when the binding of the protein to the surface is specific.<sup>3–10</sup>

Binding specificity is particularly important for antibody–antigen assays that are used in medical diagnostic tools, commonly requiring the immobilization of antibodies (ABs) on the sensor

surface.<sup>11,12</sup> Control over AB orientation is in this case of the utmost importance, since this determines for a large part the effectiveness of the ABs to detect antigens.<sup>13–18</sup> One way to

- (3) Turková, J. *J. Chrom. B* **1999**, *722*, 11–31.
- (4) Biebricher, A.; Paul, A.; Tinnefeld, P.; Götzhäuser, A.; Sauer, M. *J. Biotechnol.* **2004**, *112*, 97–107.
- (5) Zhang, K.; Diehl, M. R.; Tirrell, D. A. *J. Am. Chem. Soc.* **2005**, *127*, 10136–10137.
- (6) Zhu, H.; Snyder, M. *Curr. Opin. Chem. Biol.* **2003**, *7*, 55–63.
- (7) Rosi, N. L.; Mirkin, C. A. *Chem. Rev.* **2005**, *105*, 1547–1562.
- (8) Niemeyer, C. M. *Angew. Chem., Int. Ed.* **2001**, *40*, 4128–4158.
- (9) Katz, E.; Willner, I. *Angew. Chem., Int. Ed.* **2004**, *43*, 6042–6108.
- (10) Tiefenauer, L.; Ros, R. *Colloids Surf. B* **2002**, *23*, 95–114.
- (11) Tang, D. Q.; Tang, D. Y.; Tang, D. P. *Bioprocess Eng.* **2005**, *27*, 135–141.
- (12) Su, C. C.; Wu, T. Z.; Chen, L. K.; Yang, H. H.; Tai, D. F. *Anal. Chim. Acta* **2003**, *479*, 117–123.
- (13) O’Shannessy, D. J.; Dobersen, M. J.; Quarles, R. H. *Immunol. Lett.* **1984**, *8*, 273–277.
- (14) Hoffman, W. L.; O’Shannessy, D. J. *J. Immunol. Methods* **1988**, *112*, 113–120.
- (15) Su, C. C.; Herron, J. N. *Langmuir* **1995**, *11*, 2083–2089.
- (16) Chang, I. N.; Lin, J. N.; Andrade, J. D.; Herron, J. N. *J. Colloid Interface Sci.* **1995**, *174*, 10–23.
- (17) Buijs, J.; White, D. D.; Norde, W. *Coll. Surf. B* **1997**, *8*, 239–249.
- (18) Chen, S.; Liu, L.; Zhou, J.; Jiang, S. *Langmuir* **2003**, *19*, 2859–2864.

<sup>†</sup> Molecular Nanofabrication Group, University of Twente.

<sup>‡</sup> Laboratory of Biophysical Engineering, University of Twente.

<sup>§</sup> Wageningen University.

(1) Spinke, J.; Liley, M.; Guder, H.-J.; Angermaier, L.; Knoll, W. *Langmuir* **1993**, *9*, 1821–1825.

(2) Wilchek, M.; Bayer, E. A. *Anal. Biochem.* **1988**, *171*, 1–32.

achieve this is by using Fc receptors, such as protein A (PA), protein G (PG), or protein A/G (PA/G).<sup>19–22</sup> In such a construction, an AB binds with its Fc fragment to PA or PG, thus presenting the Fab fragments of the AB toward the solution, which thus become capable of binding antigens present in the solution.

AB-coated substrates have also been used for the adhesion and detection of cells.<sup>23–28</sup> Lymphocytes for instance, are key indicators for the diagnosis and the monitoring of malignancies, autoimmune disorders, and infections.<sup>29</sup> Lymphocytes can be divided into (i) natural killer cells, (ii) CD19<sup>+</sup> B cells, and (iii) CD3<sup>+</sup> T cells. The latter can be subdivided into CD4<sup>+</sup> T cells and CD8<sup>+</sup> T cells.<sup>29</sup> The enumeration of CD4<sup>+</sup> T-lymphocytes is essential for monitoring, for example, the infection stage of the human immunodeficiency virus (HIV) and the HIV stage of patients. For children, the CD4<sup>+</sup>/CD8<sup>+</sup> ratio is also required.<sup>30</sup>

Flow cytometry is the preferred method for CD4<sup>+</sup> enumeration, because it is very efficient and accurate. However, application of this expensive technology in resource-poor countries is a limiting factor. Cell enumeration methods based on surface detection techniques have been described.<sup>23–28</sup> The advantage is that these are more cost-effective, and the results obtained can be easily quantified. Most of the AB surfaces used for this purpose are nonspecifically immobilized, which has an effect on the total number of cells that can be bound, and thus on the detection limit.

Here we target the specific immobilization of ABs and the use of such AB-coated substrates for the development of CD3<sup>+</sup> cell count systems. To achieve the specificity, we employ the supramolecular host–guest chemistry of self-assembled monolayers (SAMs) of  $\beta$ -cyclodextrin ( $\beta$ CD). Such monolayers, also called molecular printboards, offer unique properties regarding control over binding affinity, specificity, and orientation.<sup>31</sup> These monolayers have been recently applied in the specific binding of some model proteins, including streptavidin (SAV).<sup>32,33</sup> The flexibility of this immobilization approach lies in the convenient design and the use of small, orthogonal, multivalent linker molecules that link the protein to the substrate in a controllable

fashion. By choosing the appropriate number and type of guest sites, it is possible to control thermodynamics, kinetics, and stoichiometry of the adsorption and desorption of multivalent molecules and assemblies at such surfaces. For example, the stepwise binding of SAV to  $\beta$ CD monolayers via a divalent linker has allowed heterofunctionalization of the immobilized SAV as shown previously.<sup>32</sup> Streptavidin monolayers on gold are extensively studied<sup>34–36</sup> and are commercially available, but these do not have the degree of control over thermodynamics, kinetics, and stoichiometry of the adsorption and desorption as achievable with the molecular printboard. We believe that the lessons that can be learned from supramolecular chemistry, in particular on self-assembly and the control over specificity, can play an instrumental role in a multidisciplinary approach toward complex protein bionanostructures and can provide a powerful and more systematic background for the development of relevant applications.

In this paper, we show that the supramolecularly immobilized SAV at  $\beta$ CD monolayers can be used for the specific attachment of ABs or their Fc fragments. Different assembly modes of ABs at surfaces are demonstrated, with the aims of studying their efficiency in AB binding and their use in cell counting. Assembly of an AB via a biotin functionality is compared to the assembly of the same AB via attachment to biotinylated PG (bt-PG). The assembly of such bionanostructures was investigated by surface plasmon resonance (SPR),<sup>37</sup> fluorescence spectroscopy, and atomic force microscopy (AFM). We show that such immobilized ABs can potentially be used in cell-count systems.

## Results and Discussion

To functionalize SAV with ABs, a biotinylated AB (bt-AB) or a biotinylated Fc receptor protein, such as protein A (PA) or protein G (PG), is needed. In the first part of this study, the assembly of biotinylated protein A (bt-PA) and the Fc fragment of a human IgG (IgG-Fc) (Chart 1) is described. The biotin functions present on PA and PG are randomly inserted via amide bonds. PA and PG, however, have respectively four and two IgG-binding sites, and therefore it is assumed that at least one of the IgG-binding sites is directed toward the solution.

The assembly process is depicted in Scheme 1.  $\beta$ -Cyclodextrin ( $\beta$ CD) is a well-known host for various small hydrophobic organic molecules in aqueous environment.<sup>38</sup>  $\beta$ CD has been modified with seven heptathioether chains<sup>39</sup> to obtain self-assembled monolayers (SAMs) on gold. Such SAMs are ordered and densely packed and have been extensively characterized.<sup>39,40</sup> Binding constants of monovalent guest (here, adamantyl, Ad) molecules to a single  $\beta$ CD cavity of these SAMs are comparable

(19) Akerstrom, B.; Brodin, T.; Reis, K.; Bjorck, L. *J. Immunol.* **1985**, *135*, 2589–2592.

(20) Janis, L. J.; Regnier, F. E. *Anal. Chem.* **1989**, *61*, 1901–1906.

(21) Larsson, A. *J. Immunol. Methods* **1990**, *135*, 273–275.

(22) Van de Winkel, J. G. J.; Capel, P. J. A. *Immunol. Today* **1993**, *14*, 215–221.

(23) Nibbering, P. H.; Leijh, P. C. J.; Van Furth, R. *J. Histochem. Cytochem.* **1985**, *33*, 453–459.

(24) Wysocki, L. J.; Sato, V. L. *Proc. Natl. Acad. Sci. U.S.A.* **1978**, *75*, 2844–2848.

(25) Chang, T.-W. *J. Immunol. Methods* **1983**, *65*, 217–223.

(26) Bouusso, P.; Michel, F.; Pardigon, N.; Bercovici, N.; Liblaur, R.; Kourilsky, P.; Abastado, J. P. *Immunol. Lett.* **1997**, *59*, 85–91.

(27) Belov, L.; De la Vega, O.; Dos Remedios, C. G.; Mulligan, S. P.; Christopherson, R. I. *Cancer Res.* **2001**, *61*, 4483–4489.

(28) Sekine, K.; Revzin, A.; Tompkins, R. G.; Toner, M. *J. Immunol. Methods* **2006**, *313*, 96–109.

(29) Janeway, C. A., Jr.; Travers, P.; Walport, M.; Shlomchik, M. J. *Immunobiology: The Immune System in Health and Disease*, 6th ed.; Garland Science: New York, 2005.

(30) Comans-Bitter, W. M.; De Groot, R.; Van den Beemd, R.; Neijens, H. J.; Hop, W. C. J.; Groeneveld, K.; Hoijskaas, H.; Van Dongen, J. J. M. *J. Pediatr.* **1997**, *130*, 388–393.

(31) Ludden, M. J. W.; Reinhoudt, D. N.; Huskens, J. *Chem. Soc. Rev.* **2006**, *11*, 1122–1134.

(32) Ludden, M. J. W.; Péter, M.; Reinhoudt, D. N.; Huskens, J. *Small* **2006**, *2*, 1192–120231.

(33) Ludden, M. J. W.; Mulder, A.; Tampé, R.; Reinhoudt, D. N.; Huskens, J. *Angew. Chem., Int. Ed.* **2007**, *46*, 4104–4107.

(34) Blankenburg, R.; Meller, P.; Ringsdorf, H.; Salesse, C. *Biochemistry* **1989**, *28*, 8214–8221.

(35) Hoffmann, M.; Muller, W.; Ringsdorf, H.; Rourke, A. M.; Rump, E.; Suci, P. A. *Thin Solid Films* **1992**, *210*, 780–783.

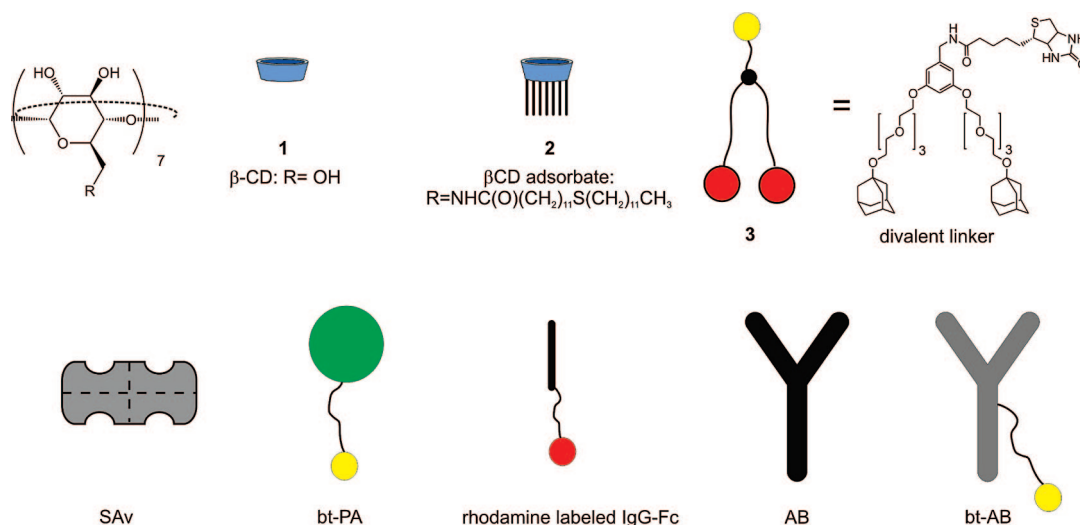
(36) Yang, N.; Su, X. D.; Tjong, V.; Knoll, W. *Biosens. Bioelect.* **2007**, *22*, 2700–2706.

(37) Knoll, W. *Annu. Rev. Phys. Chem.* **1998**, *49*, 569–638.

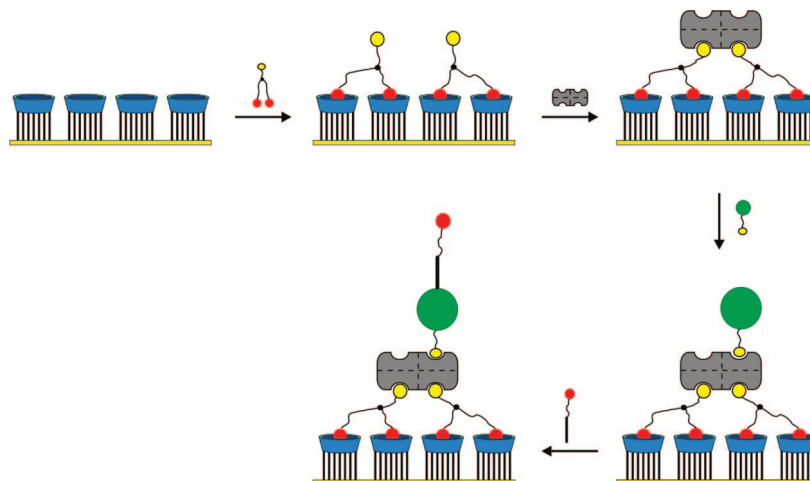
(38) Rekharsky, M. V.; Inoue, Y. *Chem. Rev.* **1998**, *98*, 1880–1901.

(39) Beulen, M. W. J.; Bügler, J.; Lammerink, B.; Geurts, F. A. J.; Biemond, E. M. E. F.; Van Leerdam, K. G. C.; Van Veggel, F. C. J. M.; Engbersen, J. F. J.; Reinhoudt, D. N. *Langmuir* **1998**, *14*, 6424–6429.

(40) Beulen, M. W. J.; Bügler, J.; De Jong, M. R.; Lammerink, B.; Huskens, J.; Schönherr, H.; Vancso, G. J.; Boukamp, B. A.; Wieder, H.; Offenhäuser, A.; Knoll, W.; Van Veggel, F. C. J. M.; Reinhoudt, D. N. *Chem. Eur. J.* **2000**, *6*, 1176–1183.

Chart 1. Building Blocks Used in This Study<sup>a</sup>

<sup>a</sup>  $\beta$ CD,  $\beta$ CD adsorbate for SAM preparation on gold, divalent adamantyl-biotin linker (3), SAV, bt-PA, rhodamine-labeled IgG-Fc, and the general structure of biotinylated antibodies.

Scheme 1. Buildup of a Bionanostructure Composed of 3, SAV, bt-PA, and Rhodamine-Labeled IgG-Fc at  $\beta$ CD Monolayers

to binding constants of these molecules to  $\beta$ CD in solution.<sup>41</sup> All guest-binding sites in the  $\beta$ CD monolayer are equivalent and independent. The multivalent<sup>31</sup> host–guest interactions allows the formation of kinetically stable assemblies, and thus local complex formation, for example, by patterning, so that these surfaces can be viewed as “molecular printboards”.<sup>42,43</sup>

First the divalent bis-Ad-biotin linker 3 is bound to the  $\beta$ CD monolayer, followed by the attachment of SAV, yielding immobilized SAV, with two biotin-binding pockets available for further functionalization.<sup>32</sup> Bt-PA is attached to these biotin-binding pockets. This protein serves as an Fc receptor, so that IgG-Fc can be attached on top. Thus, in this assembly scheme, three orthogonal, noncovalent interactions are present:  $\beta$ CD-Ad, SAV-biotin, and bt-PA-IgG-Fc.

When considering the assembly of different proteins on top of each other, the sizes and shapes of the different proteins need to be taken into account. When SAV (58 kDa; 2.5 nm  $\times$  3 nm

$\times$  5 nm) is immobilized via two biotin-binding pockets to a surface, the spacing between the remaining free biotin-binding pockets is about 2 nm.<sup>44</sup> PA and PG are globular proteins with sizes of 42 and 22 kDa, respectively, corresponding to diameters of  $\sim$ 5 and  $\sim$ 4 nm. This means that these Fc receptors can only bind to SAV in a 1:1 ratio. ABs are even larger ( $\sim$ 150 kDa) and are Y-shaped, thus the binding ratio of AB to Fc receptor (and SAV) can never be larger than 1.

SPR<sup>37</sup> experiments showed that both bt-PA and IgG-Fc have significant nonspecific interactions with  $\beta$ CD monolayers (Figure 1a, yellow line, and 1b, light blue line) in phosphate buffered saline (PBS), as the SPR curves show considerable adsorption which is only partially reversible by rinsing with 10 mM  $\beta$ CD. Adding 1 mM  $\beta$ CD to the PBS buffer during adsorption appeared to be sufficient to minimize nonspecific adsorption of bt-PA to the  $\beta$ CD monolayers (Figure 1a, red line), but not to inhibit nonspecific interactions of IgG-Fc to  $\beta$ CD monolayers (Figure 1b, dark blue line). In contrast,  $1 \times 10^{-7}$  M BSA was efficient in inhibiting nonspecific interactions of IgG-Fc at the

(41) De Jong, M. R.; Huskens, J.; Reinhoudt, D. N. *Chem. Eur. J.* **2001**, *7*, 4164–4170.

(42) Reinhoudt, D. N.; et al. *Angew. Chem., Int. Ed.* **2004**, *43*, 369–373.

(43) Huskens, J.; Deij, M. A.; Reinhoudt, D. N. *Angew. Chem., Int. Ed.* **2002**, *41*, 4467–4471.

(44) Ding, Z.; Fong, R. B.; Long, C. L.; Stayton, P. S.; Hoffmann, A. S. *Nature* **2001**, *411*, 59–62.

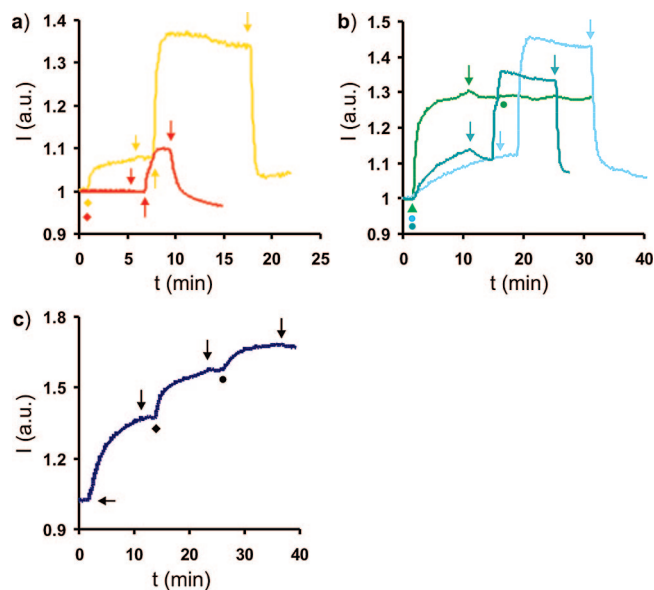


**Figure 1.** SPR sensograms representing the nonspecific adsorption of bt-PA (a) and IgG-Fc (b) to  $\beta$ CD SAMs, and the buildup of a bionanostructure consisting of divalent linker (**3**), SAV, bt-PA, and IgG-Fc according to Scheme 1 (c): (a) bt-PA in PBS (yellow), bt-PA adsorption in 1 mM  $\beta$ CD in PBS (red); (b) IgG-Fc in PBS (light blue), IgG-Fc adsorption in 1 mM  $\beta$ CD in PBS (dark blue), BSA adsorption followed by IgG-Fc adsorption in PBS (green); (c) assembly of SAV, bt-PA, and IgG-Fc onto a 3-covered  $\beta$ CD SAM. Symbols indicate switching the flow to ( $\downarrow$ ) buffer, ( $\uparrow$ ) 10 mM  $\beta$ CD in PBS, ( $\bullet$ ) IgG-Fc, ( $\leftarrow$ ) SAV, ( $\blacklozenge$ ) bt-PA, and ( $\blacktriangle$ ) BSA.

$\beta$ CD monolayer (Figure 1b, green line), as the SPR curve showed the strong adsorption of BSA but no signal increase after subsequent exposure to the IgG-Fc solution. On the basis of these results, it was expected and confirmed (see later) that SAV can fulfill a similar blocking function in the assembly of the bionanostructure. For this reason, it is sufficient to use 1 mM  $\beta$ CD in the adsorption medium to suppress nonspecific interactions. This is preferred over a blocking step with BSA as this may interfere with subsequent surface adsorption steps, while the addition of  $\beta$ CD to the adsorption medium leaves the surface binding sites unchanged.

To build the complete assembly based on specific interactions, as depicted in Scheme 1, a  $\beta$ CD SAM on gold was subsequently immersed in solutions of **3**, SAV, bt-PA, and IgG-Fc, while in between these steps PBS buffer containing 1 mM  $\beta$ CD was flowed over the substrate to avoid protein–protein interactions in solution. Figure 1c shows an SPR sensogram in which the protein adsorption steps of this assembly process are represented. After returning to PBS containing 1 mM  $\beta$ CD, it is evident that the bionanostructure remained at the surface.

Patterned bionanostructures according to Scheme 1 were obtained by microcontact printing ( $\mu$ CP) of the divalent linker **3**<sup>32</sup> onto  $\beta$ CD monolayers on glass,<sup>45</sup> followed by flowing SAV, bt-PA, BSA, and IgG-Fc over the sample (Figure 2, left). Nonspecific interactions in the nonpatterned areas were minimized by blocking with BSA. For fluorescence imaging of the final structure, the IgG-Fc was labeled with lissamine–rhodamine according to a literature procedure.<sup>46</sup> Subsequently bt-PA was flowed over the substrate in the presence of 1 mM  $\beta$ CD, followed by BSA and IgG-Fc. Figure 2 (left) confirms the

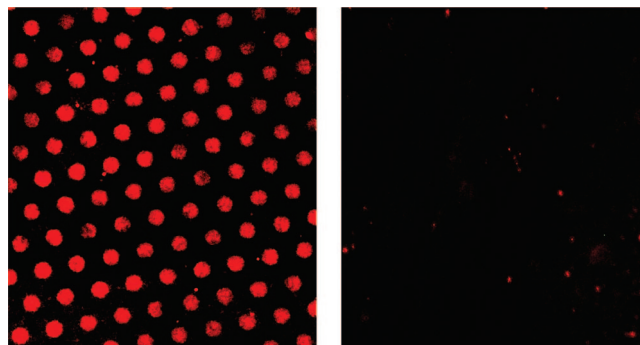


**Figure 2.** Fluorescence images of a patterned bionanostructure prepared by microcontact printing of the divalent linker (**3**), followed by adsorption of SAV, bt-PA, and rhodamine-labeled IgG-Fc (left; Scheme 1), and of a sample for which bt-PA was omitted (right).

selective buildup of the SAV-PA-IgG-Fc bionanostructure on the surface only in the areas where the linker **3** was printed in the first step.

Reference experiments in which each time one of the building blocks was omitted (linker, SAV, or bt-PA), showed no fluorescent patterns at all, indicating the need for all components of this system to form the assembly. In particular the absence of fluorescence in the case when bt-PA was omitted is illustrative (Figure 2, right). It shows that the fluorescently labeled IgG-Fc does not interact with SAV directly and thus that SAV also suppresses nonspecific interactions of IgG-Fc to  $\beta$ CD monolayers, similar to the blocking function of BSA in the empty  $\beta$ CD SAM areas (see above). The SPR and fluorescence experiments prove that all assembly steps occur in a specific manner, thereby showing that it is possible to attach bionanostructures to the molecular printboard consisting of different proteins. The specificity shown in this experiment is very important when targeting diagnostic applications, for example, antibody assays or cell count systems as described later.

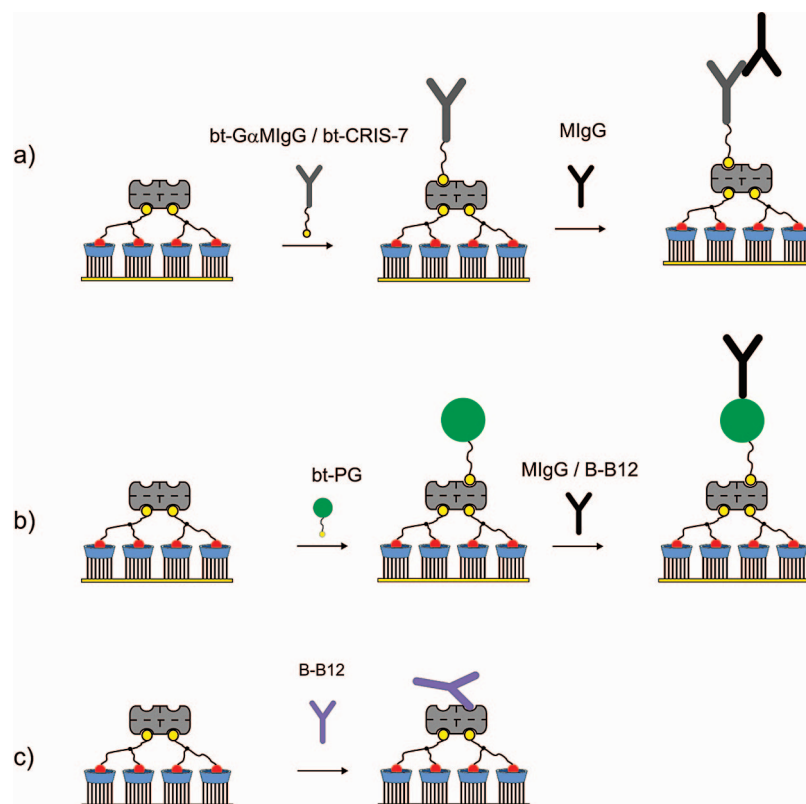
Scheme 2 presents the attachment of complete ABs via two different assembly methods. The first (Scheme 2a) employs biotinylated goat antimouse IgG (bt-G $\alpha$ MIgG) which is bound through its biotin functionality to the SAV layer at the SAV-3-covered  $\beta$ CD monolayer. Mouse IgG (MIgG) can subsequently interact with the first AB. In Scheme 2b, a route is depicted in which the binding of MIgG is regulated via the attachment of bt-PG.

SPR experiments were performed to investigate possible nonspecific interactions of the different ABs to  $\beta$ CD monolayers. As expected from the results with IgG-Fc, also the complete ABs showed nonspecific interactions to the molecular printboard, as indicated by the strong SPR signal increase shown in Figure 3a upon adsorption of bt-G $\alpha$ MIgG. The SPR sensograms displayed in Figure 3b and 3d indicate that adding 1 mM  $\beta$ CD to the PBS buffer did not eliminate nonspecific attachment of the ABs, as also in these cases adsorption of the ABs is apparent from the SPR curves. However, when BSA was preadsorbed (Figure 3c,e), no SPR signal increase occurred upon exposure to solutions of the ABs. This has been noted before for the IgG-Fc as well (see above). Similarly as indicated above for the Fc fragment, we assume that also SAV inhibits nonspecific interactions of the whole IgGs with the  $\beta$ CD SAMs within the bionanostructures.

SPR sensograms of the assembly formation according to Scheme 2 are depicted in Figure 4. In Figure 4a the assembly consisting of bt-G $\alpha$ MIgG and MIgG is depicted (Scheme 2a).

(45) Onclin, S.; Mulder, A.; Huskens, J.; Ravoo, B. J.; Reinhoudt, D. N. *Langmuir* **2004**, *20*, 5460–5466.

(46) Brinkley, M. *Bioconj. Chem.* **1992**, *3*, 2–13.

Scheme 2. AB Bionanostructures to  $\beta$ CD Monolayers Covered with **3** and SA $v^a$ 

<sup>a</sup> Adsorption of bt-G $\alpha$ MIgG or bt-CRIS-7 and the subsequent attachment of MIgG to bt-G $\alpha$ MIgG (a), adsorption of bt-PG and the subsequent attachment of MIgG or B-B12 (b), and the (nonspecific) adsorption of B-B12 onto SA $v$ . Schemes a (bt-G $\alpha$ MIgG + MIgG) and b (bt-PG + MIgG) apply to the study on the assembly of ABs while the attachments of bt-CRIS-7 (a) and B-B12 (b, c) apply to the cell adhesion studies.

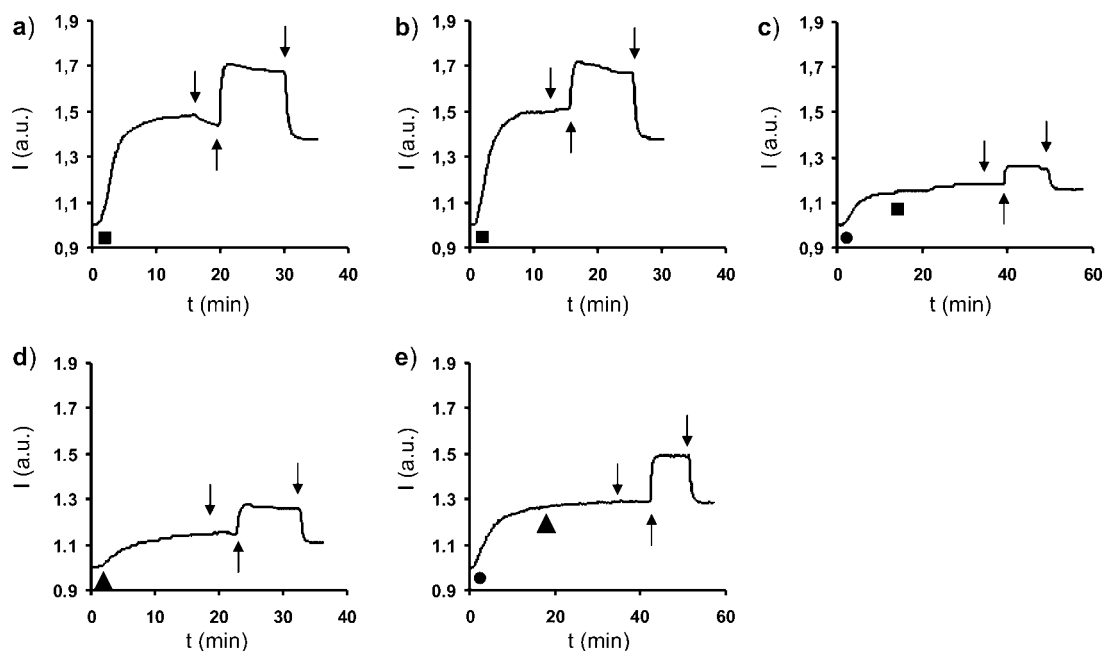


**Figure 3.** SPR sensograms displaying the nonspecific attachment of two different antibodies at  $\beta$ CD SAMs: adsorption of bt-G $\alpha$ MIgG in PBS, in the absence (a) or the presence (b) of 1 mM  $\beta$ CD, or with preceding adsorption of BSA (c); adsorption of MIgG in PBS containing 1 mM  $\beta$ CD (d) or with preceding adsorption of BSA (e). Symbols indicate switching the flow to (t) 10 mM  $\beta$ CD, (↓) buffer with (b,d) or without (a,c,e) 1 mM  $\beta$ CD, (●) BSA, (■) bt-G $\alpha$ MIgG, and (▲) MIgG.

The SPR signal increased upon AB flow, but this increase was rather small. For example, the signal increase upon adsorption of SA $v$  was larger than for the ABs, while the ABs are substantially larger (150 kDa, compared to 58 kDa for SA $v$ ).

Also compared to adsorption of only an Fc fragment (Figure 1c), the SPR signal increase for a complete AB was comparable in size, while the MW of the AB is considerably higher. Therefore this indicates that the immobilized ABs do not have

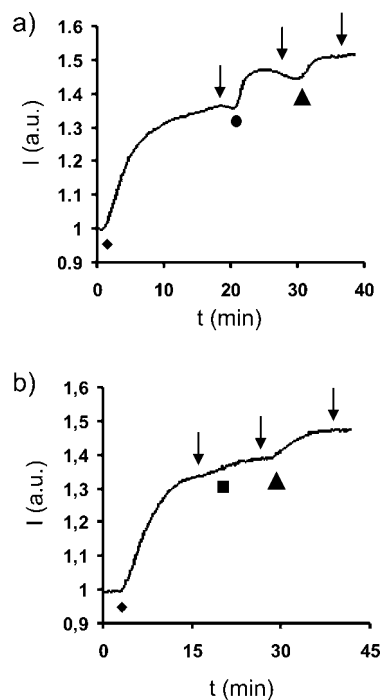


**Figure 4.** SPR sensograms of the assembly of antibodies at 3-covered  $\beta$ CD SAMs via the routes shown in Scheme 2a,b. Symbols indicate ( $\blacklozenge$ ) SAv, ( $\blacklozenge$ ) PBS containing 1 mM  $\beta$ CD, ( $\bullet$ ) bt-G $\alpha$ MIgG, ( $\blacktriangle$ ) MIgG, and ( $\blacksquare$ ) bt-PG.

**Table 1.** Heights Measured in AFM Scratching Experiments on Fully Protein-Covered  $\beta$ CD Monolayers Made According to Scheme 2

assembly	height (nm)
3•SAv	2.5
3•SAv•bt-G $\alpha$ MIgG	4
3•SAv•bt-G $\alpha$ MIgG•MIgG	5.7
3•SAv•bt-PG	3.5
3•SAv•bt-PG•MIgG	5.9

a dense packing. Also the attachment via bt-PG as shown in Figure 4b appeared feasible, however also in this case the increase in SPR signal corresponding to the adsorption of AB remained rather low, indicating that also in this case the resulting AB layer is not dense.

AFM experiments were performed to investigate the different assembly steps. Five samples were prepared according to Schemes 2a and b. The substrates were fully covered with proteins, and a small scratch with the AFM tip was made on the samples from which the heights of the protein layers could be measured (Table 1).

The height of SAv was the same as measured in the patterning AFM experiments on  $\beta$ CD monolayers described previously.<sup>32</sup> The height increments after the different adsorption steps were lower than expected based on the sizes of the different proteins, especially for the AB adsorption steps, confirming the SPR results. This observation may be due to the high compressibility of the adsorbed proteins, and partly because the packing of the ABs at the surface is not dense, owing to the different sizes and shapes of the proteins present in the bionanostructures at the  $\beta$ CD monolayers. It should be noted that the AB packing density is higher in the case of bt-PG compared to G $\alpha$ MIgG, as witnessed by the larger height increase upon AB adsorption in the former case. Moreover, the specific binding of a particular antibody with its antigen is such that the major part of the

antigen is located next to the antibody binding site, which would result in only a limited increase in the total height of the complex. Nevertheless, the results clearly indicate that also complete ABs can be immobilized using a supramolecular assembly scheme. Especially the immobilization scheme via PG is important, since it allows control over the orientation of ABs.

In this study, we target the use of AB-coated surfaces for cell counting applications. A major application is the counting of lymphocytes, in particular in the follow up of HIV-infected persons. Most available cell count methods are rather expensive, and the read-out is far from easy. Therefore, these systems are not used in resource-constrained countries. A target is therefore to develop an inexpensive and easily read cell-count system for CD3<sup>+</sup> lymphocytes. For such an application, two main issues need to be addressed: (i) the specificity of cell adhesion as a function of the method of AB immobilization and (ii) the verification of whether the relation between the number of seeded cells and the number of actually counted cells is linear. Both issues are subsequently addressed.

For the attachment of CD3<sup>+</sup> lymphocytes to surfaces, two monoclonal ABs (MABs) were immobilized, one from a CRIS-7 clone and one from a B-B12 clone. The MAB from the CRIS-7 clone was, on average, monobiotinylated for direct attachment to SAv (Scheme 2a, first adsorption step). These biotin moieties can be attached randomly to different free amino groups present at the outside of the MAB. Therefore, not all Fab fragments will be directed upward. The B-B12 MAB did not have a biotin functionality and was therefore assembled via an Fc receptor (Scheme 2b). The advantage of using an Fc receptor is that the Fc part of the AB is directed toward the surface, and the Fab part, capable of binding antigens, is directed toward the solution interface. Thus, the surface density of Fab portions which are directed upward is potentially enhanced.

Dot-blot experiments<sup>47</sup> (see Experimental Section) were performed to check which of the Fc receptor proteins (PA or PG) is best suitable to bind the B-B12 MAB. From these experiments, it became clear that bt-PA did not bind the B-B12 MAB very strongly. However, bt-PG appeared to have a strong affinity for the B-B12 MAB and was therefore used in subsequent experiments for preparing the bionanostructures according to Scheme 2b.

The binding of the MABs bt-CRIS-7 and B-B12 to SAv layers at  $\beta$ CD monolayers according to Scheme 2a and 2b, respectively, was investigated by SPR spectroscopy (Figure 5). For the experiment with the bt-CRIS-7 MAB, SAv was flowed over the substrate. Subsequently, bt-CRIS-7 ( $10^{-7}$  M in 1 mM  $\beta$ CD in PBS) was flowed over the surface. Figure 5a shows a relatively high signal for the binding of the CRIS-7 MAB, in particular when compared to the adsorption of bt-G $\alpha$ MIgG (Figure 4a).

For the structures consisting of the B-B12 MAB, SAv and bt-PG were adsorbed, followed by a flow of  $10^{-7}$  or  $10^{-6}$  M of the B-B12 MAB (Figure 5b and 5c, respectively). When this is compared to the binding of CRIS-7 at equal AB concentration (Figure 5a and 5b), it appeared that the binding of B-B12 was significantly lower, but still more than the adsorption of MIgG (either via bt-G $\alpha$ MIgG or bt-PG, Figure 4). This can potentially be attributed to a slower association kinetics for the B-B12 MAB. Therefore, a higher MAB concentration ( $10^{-6}$  M) was attempted (Figure 5c) which indeed resulted in enhanced

(47) Dot blot protocol. <http://www.Abcam.com/technical> (accessed September 2006).

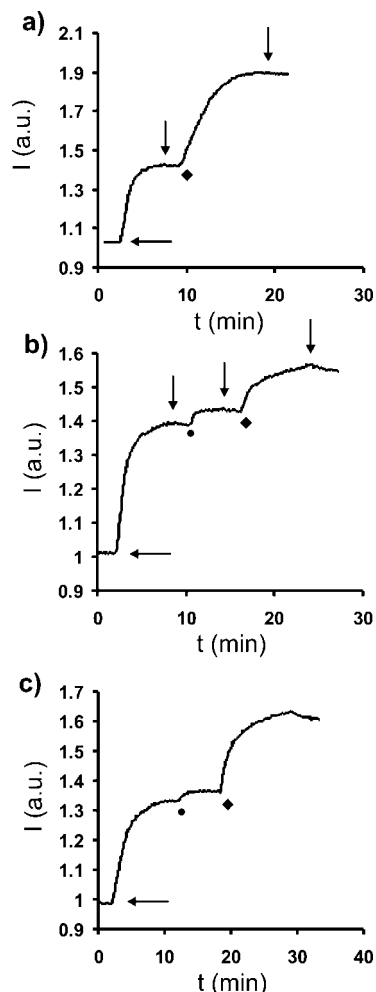


**Figure 5.** SPR sensograms of the adsorption of SAV to  $\beta$ CD SAMs, followed by the adsorption of the bt-CRIS 7 MAB (a; Scheme 2a) or bt-PG with subsequent B-B12 MAB adsorption (Scheme 2b) from a  $10^{-7}$  M (b) and a  $10^{-6}$  M solution of the B-B12 MAB (c). Symbols indicate SAV ( $\leftarrow$ ), bt-PG ( $\bullet$ ), bt-CRIS-7 (a) or B-B12 (b,c) MAB ( $\blacklozenge$ ), PBS + 1 mM  $\beta$ CD ( $\blacklozenge$ ).

binding, but still not as much as observed for the CRIS-7 MAB. Potentially, this binding enhancement can also be attributed to nonspecific binding of B-B12, even though it was shown earlier that SAV (like BSA) can suppress nonspecific interactions of Fc fragments and even complete ABs. Also it will be shown later that the specificity of cell binding at this higher B-B12 concentration is comparable to specificity obtained at the lower concentration and considerably better than when using nonspecifically adsorbed B-B12.

For studying the specificity of lymphocyte cell adhesion, CRIS-7 and B-B12 MAB surface assemblies were prepared according to Scheme 2a (first adsorption step) and according to 2b and 2c, respectively. To study nonspecifically bound B-B12 surfaces (Scheme 2c), B-B12 was flowed directly over SAV $\cdot$ 3 on a  $\beta$ CD SAM. After attachment of the proteins the samples were rinsed carefully with PBS. Thereafter, 200  $\mu$ L of a suspension of lymphocytes ( $1 \times 10^5$  cells/ $\mu$ L), which had been stained with Hoechst 33342 and CD4FITC, was placed on the substrate, and the cells were incubated for 30 min at room temperature in the dark. Hoechst 33342 is a general DNA-binding dye, coloring all cells present at the surface. CD4FITC, CD3PE, and CD8APC are dye-labeled ABs that are directed to specific proteins present in the cell membrane (CD4, CD3, and

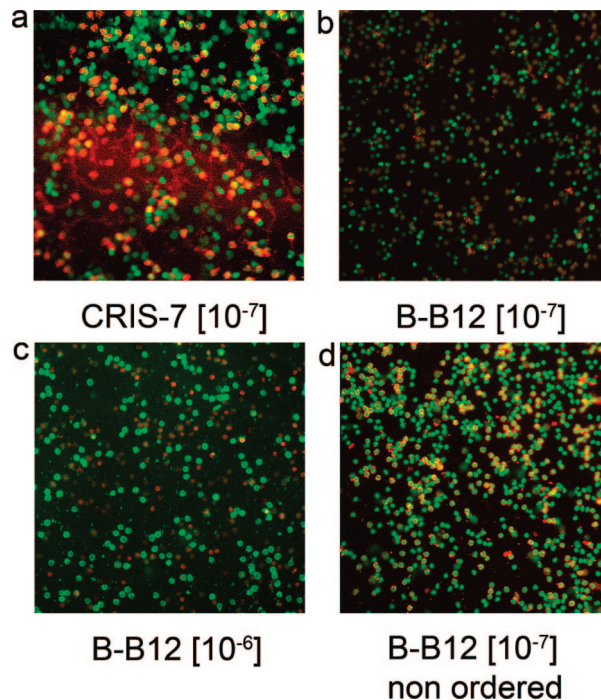


**Figure 6.** Overlays of fluorescence microscopy images for the different cell adsorption experiments according to Scheme 2 prepared from  $10^{-7}$  M btCRIS-7 (a, Scheme 2a),  $10^{-7}$  M (b) and  $10^{-6}$  M (c) B-B12 onto bt-PG (Scheme 2b), and  $10^{-7}$  M B-B12 onto SAV (d, Scheme 2c). Hoechst 33342 is depicted in green, and CD4FITC is depicted in red.

CD8, respectively). Therefore, cells colored with these dyes indicate specific immobilization. After removal of the cell suspensions, and a washing procedure (see Experimental Section), surface-immobilized cells were detected by fluorescence microscopy. The specificity of the cell adsorption can be determined by comparison of the overlay of the images of CD4FITC (displayed in red) and Hoechst 33342 (displayed in bright green/yellow) (Figure 6). Cells which are only stained with Hoechst 33342 are displayed in bright green/yellow and are regarded as being nonspecifically adsorbed. The cells stained both by Hoechst 33342 and CD4FITC are displayed in darker green/red and are regarded as being specifically immobilized.

Specific cell adsorption at the bt-CRIS-7 substrate (Scheme 2a) was only 40%, and 45% at the substrate in which B-B12 MAB was nonspecifically adsorbed (without bt-PG at SAV; Scheme 2c). In contrast, the samples in which the B-B12 MAB was bound specifically through bt-PG (Scheme 2b) showed the highest numbers of specifically adsorbed cells (65% and 68% for the samples created from the  $10^{-6}$  and  $10^{-7}$  M B-B12 solutions, respectively). The better cell adhesion specificity in these cases is attributed to a more favorable MAB orientation induced bt-PG, allowing a higher fraction of the B-B12 MABs to interact with a cell membrane-expressed antigen. Since the results from cell adsorption at the specifically adsorbed B-B12 surfaces prepared from  $10^{-7}$  and  $10^{-6}$  M concentrations of B-B12 seemed to give comparable results, cell count linearity studies (below) were performed on the B-B12 surface prepared from a  $10^{-7}$  M solution.

For the linearity study, four substrates onto which B-B12 was immobilized via bt-PG (Scheme 2b) were prepared, and each sample was incubated for 30 min at room temperature in the dark, with a different concentration of lymphocytes on each sample. The concentration of lymphocytes, as determined by flow cytometry, contained in total 8500 lymphocytes/ $\mu$ L, of



**Table 2.** Results of Linearity Studies on Four Samples Prepared According to Scheme 2b: Numbers of Seeded CD3<sup>+</sup> Cells, Theoretically Expected CD3<sup>+</sup> Cells Per Image, and the Actually Immobilized Cells As Visualized by Fluorescence Microscopy Imaging

sample	Seeded cells (#/ $\mu$ L)	Expected cells (#/image) <sup>a</sup>	Immobilized cells (#/image)
1	2016	1199	1253
2	1005	598	424
3	503	299	159
4	248	148	43

<sup>a</sup>The numbers of expected cells per image are based on the assumption of complete cell adsorption from the cell suspension (height 1.045 mm) standing on the image area (0.675  $\times$  0.843 mm<sup>2</sup>).

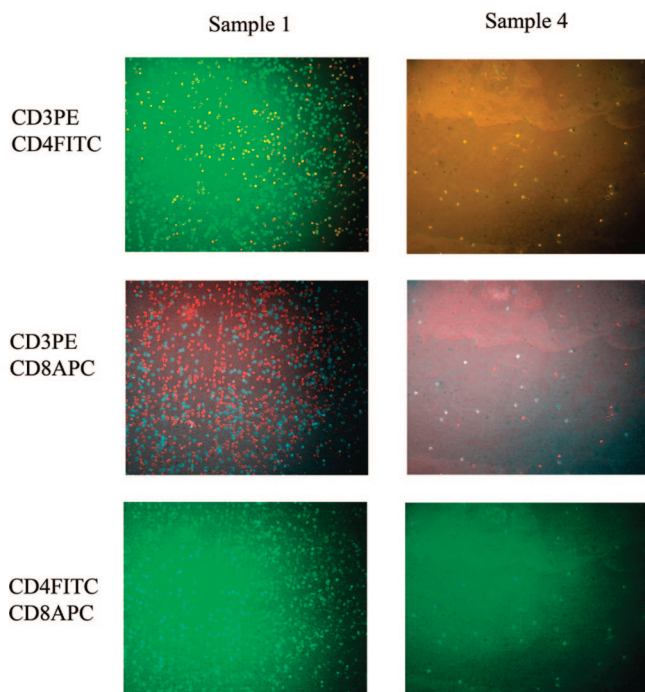


**Figure 7.** Fluorescence microscopy images of the linearity studies performed on B-B12 MAB samples prepared according to Scheme 2b incubated at high (sample 1) and 8-fold lower (sample 4) cell concentrations (see Table 2). CD3<sup>+</sup> cells are depicted in red, CD4<sup>+</sup> cells are depicted in green, and CD8<sup>+</sup> cells are depicted in cyan.

which 6200 were CD3<sup>+</sup> T cells/ $\mu$ L (3500 CD3<sup>+</sup>CD4<sup>+</sup> T cells/ $\mu$ L and 2700 CD3<sup>+</sup>CD8<sup>+</sup> T cells/ $\mu$ L). Four lymphocyte suspensions were prepared by dilution of the original cell suspension with PBS. From these numbers the expected numbers of cells per image can be calculated (Table 2).

The cell suspensions were removed after 30 min from the substrate, followed by rinsing. Thereafter, cells were incubated with a solution containing Hoechst 33342, CD3PE, CD4FITC, and CD8APC to color the cells in different manners, as described above. Subsequently, fluorescence images were recorded in three different spots on the sample, from CD3PE (depicted in red/yellow), CD4FITC (depicted in green), and CD8APC (depicted in cyan). In Figure 7, overlay images are presented of the samples with the highest and the lowest cell concentrations. From these overlay images the numbers of CD3<sup>+</sup>CD4<sup>+</sup> and CD3<sup>+</sup>CD8<sup>+</sup> cells can be estimated. From the first row of images the number of CD3<sup>+</sup> cells can be determined by counting the yellow/red-looking cells. From the images displayed in the second row, the number of CD8<sup>+</sup> cells can be determined by counting the cyan colored cells. In the third row

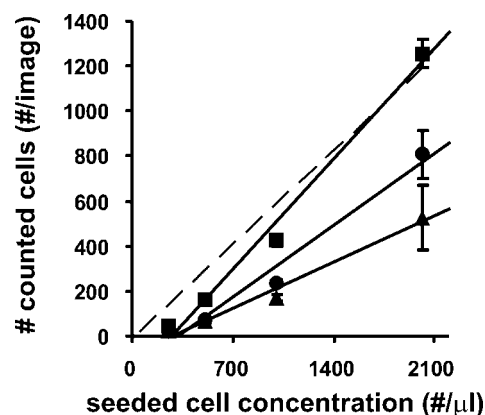


**Figure 8.** Linearity plots showing the number of counted cells versus the number of seeded cells of lymphocyte incubation performed on B-B12 MAB samples prepared according to Scheme 2b: CD3<sup>+</sup> cells (●), CD3<sup>+</sup>CD4<sup>+</sup> cells (▲), and CD3<sup>+</sup>CD8<sup>+</sup> cells (■). Error bars indicate the standard deviations of cell numbers counted in three different areas on the same samples. The solid lines represent linear fits, while the dotted line shows the theoretical number of cells versus the seeded number of cells.

overlay images are presented from which again the total number of cells can be determined, which should be similar to the number of CD3<sup>+</sup> cells plus the number of CD8<sup>+</sup> cells. The specificity of the cell adsorption measured on all substrates is similar, and comparable to the experiments shown above.

To determine if the relation between the adsorbed cells in the different experiments is linear, the counted numbers of CD3<sup>+</sup>, CD3<sup>+</sup>CD4<sup>+</sup>, and CD3<sup>+</sup>CD8<sup>+</sup> cells were plotted versus the number of seeded cells (Figure 8). Each data point in this graph represents the average number of cells counted on three different images from the same surface. The solid lines represent linear fits of these data points.

In Figure 8, the dashed line represents the theoretical linear relationship between seeded cells and counted cells. The expected numbers of cells were calculated by assuming that all CD3<sup>+</sup> T cells are captured on a surface, which is 60% of the total number of cells put on top of the sample (see Experimental Section). The theoretical number of captured cells is not reached fully except for the case with the highest number of seeded cells, as evidenced by the offset of the linear fits, which indicate that cells will not be detected anymore when the seeded number of cells is lower than 265–320 per  $\mu$ L. However, all cell species at the surface show an approximately linear relationship (Figure 8), suggesting that the molecular printboard can potentially be used for the detection of CD3<sup>+</sup> cells by ABs.

## Conclusions

We have shown that (complex) bionanostructures can be assembled, in patterned and nonpatterned fashions, in a specific manner to the molecular printboard via orthogonal linkers. In this assembly scheme, different interaction types were used: host–guest, protein–ligand, and protein–protein interactions. The specificity of binding was shown very clearly in the patterning experiments in which three different proteins were sequentially and specifically adsorbed to a  $\beta$ CD monolayer via a small molecule linker.

This manner of assembling bionanostructures on the surface was applied in the buildup of structures that are able to serve as platforms for specific cell immobilization. From these studies an approximately linear lymphocyte immobilization behavior was observed, indicating that this system can potentially be applied in cell count systems. Since every step in the build-up

of these complex bionanostructures is specific, it can be employed in different systems in which specificity is of utmost importance, such as diagnostic applications.

Future work will deal with improving the specificity of antibody adhesion, for example using the method described before using a nonspecific adsorption-suppressing ethylene glycol derivative. This should allow specific antibody adsorption in media that are more relevant for biosensing, for example, blood serum. Also improved specificity for cell immobilization is an important target, so that the systems described here can be further developed into low-cost cell-count systems.

## Experimental Section

**General.** All chemicals were used as received. Compounds **2**, **3**, and  $\beta$ CD-heptamine were synthesized as reported before.<sup>32,39,48</sup> SA<sub>v</sub>, IgG-FITC from human serum, bt-PA, bt-PG, and IgG-Fc from human serum were obtained from Sigma Aldrich. MAB to CD3 from clone CRIS-7 (isotype Mouse IgG2a, $\kappa$ ; 0.526 mg/ml) and MAB to CD3 from clone B-B12 (isotype IgG1,  $\kappa$ ; 3.385 mg/ml) were obtained from the Antibodystore. Biotinylation of CRIS-7 was performed by Immunicon. Hoechst 33342 for DNA staining was obtained from Molecular Probes, Invitrogen. CD3PE, CD4FITC, and CD8APC were obtained from BD Bioscience. Mouse IgG, whole molecule, and biotinylated goat-antimouse IgG were obtained from Jackson ImmunoResearch Laboratories, West Grove. The functionalization of IgG-Fc (Sigma-Aldrich) with rhodamine was performed according to literature procedures. After labeling, the protein/rhodamine ratio was on average 1:2.<sup>46</sup> The luminol/enhancer solution was obtained from Pierce. Throughout all experiments 10 mM phosphate buffered saline (PBS) at pH 7.5 containing 150 mM NaCl was used.

**Monolayer Preparation.** Gold substrates for SPR (BK7 glass/2–4 nm Ti/50 nm Au), XPS (BK 7 glass/2–4 nm Ti/200 nm Au) and AFM (Si wafer/2–4 nm Ti/20 nm Au) were obtained from Ssens B.V., Hengelo, The Netherlands. Gold substrates were cleaned by dipping them in piranha (1:3 mixture of concentrated H<sub>2</sub>SO<sub>4</sub> and 30% H<sub>2</sub>O<sub>2</sub>) for 5 s. (*Warning*: piranha should be handled with caution; it can detonate unexpectedly.) After thorough rinsing with Millipore water, they were placed for 10 min in absolute EtOH to remove the oxide layer. Subsequently the substrates were placed in a freshly prepared 0.1 mM solution of  $\beta$ CD heptathioether **2** for 16 h at 60 °C.<sup>39</sup> The samples were subsequently rinsed three times with CHCl<sub>3</sub>, EtOH, and Millipore water.  $\beta$ CD monolayers on glass were prepared as described earlier.<sup>45</sup> All solvents used in the monolayer preparation were of p.a. (pro analysi) grade.

**Protein Immobilization at the Molecular Printboard for SPR, Fluorescence Studies, AFM, and Cell Immobilization.** A  $\beta$ CD monolayer was immersed in a 1 mM aqueous solution of **3**. Subsequently, the substrate was rinsed with water, dried in a stream of N<sub>2</sub>, and further processes could be performed. In between different protein assembly steps, PBS buffer containing 1 mM  $\beta$ CD was flowed over the substrate to avoid protein–protein interactions in solution.

**SPR.** SPR measurements were performed on a Resonant Probes GmbH SPR instrument. The instrument consists of a HeNe laser (JDS Uniphase, 10 mW,  $\lambda = 632.8$  nm) of which the laser light passes through a chopper that is connected to a lock-in amplifier (EG&G 7256). The modulated beam is directed through two polarizers (OWIS) to control the intensity and the plane of polarization of the light. The light is coupled via a high index prism (Scott, LaSFN9) in the Kretschmann configuration to the backside of the gold-coated substrate which is optically matched through a refractive index matching oil (Cargille; series B;  $n_D^{25\text{ }^\circ\text{C}} = 1.700 \pm 0.0002$ ) at the prism, mounted on a  $\theta$ – $2\theta$  goniometer, in contact with a Teflon cell with a volume of 39  $\mu$ L and a diameter of 5 mm. The light that leaves the prism passes through a beam splitter,

subsequently, the s-polarized light is directed to a reference detector, and the p-polarized light passes through a lens which focuses the light onto a photodiode detector. Laser fluctuations are filtered out by dividing the intensity of the p-polarized light ( $I_p$ ) by the intensity of the s-polarized light ( $I_s$ ). All measurements were performed at a constant angle by reflectivity tracking. A Reglo digital MS-4/8 flow pump from Ismatec with four channels was used. In this flow pump, Tygon R3607 tubings with an inner diameter of 0.76 mm were used, obtained from Ismatec.

The SPR experiments were performed under a continuous flow of 0.5 mL/min. Experiments were started after the baseline was stable. When the solution had to be changed, the pump was stopped, and immediately after changing the solution the pump was switched on again. Concentrations of proteins that were flowed during experiments were  $1 \times 10^{-7}$  M, unless stated otherwise.

For the SPR experiments in which the nonspecific adsorption of bt-PA and IgG-Fc was studied, the proteins were flowed at 0.5 mL/min over the surface at a concentration of  $1 \times 10^{-7}$  M in PBS. Subsequently, 10 mM  $\beta$ CD in PBS was flowed over the surface at the same flowrate, followed by PBS. For both bt-PA and IgG-Fc, the same procedure was repeated with the difference that the PBS buffer was replaced with a PBS buffer containing 1 mM  $\beta$ CD. For IgG-Fc an experiment was performed in which prior to the IgG-Fc flow BSA was adsorbed to the surface from a  $1 \times 10^{-7}$  M BSA solution in PBS. A 10 mM  $\beta$ CD rinse in PBS was not applied in this case. Every protein flow was followed by a flow of 1 mM  $\beta$ CD in PBS before switching to 10 mM  $\beta$ CD in PBS.

For the SPR experiment in which the whole assembly was adsorbed to the surface, a  $\beta$ CD SAM on gold was immersed in a  $10^{-5}$  M aqueous solution **3** for 15 min, followed by rinsing with Millipore water. After that, the substrate was assembled in the SPR setup. The SPR experiment was performed in 1 mM  $\beta$ CD in PBS at a flowrate of 0.5 mL/min. Every protein flow was followed by a flow of 1 mM  $\beta$ CD in PBS.

The SPR experiments for the determination of the nonspecific interactions between bt-G $\alpha$ MlgG and the molecular printboard and MlgG and the molecular printboard were performed as described for bt-PA and IgG-Fc at a concentration of  $1 \times 10^{-7}$  M and at a flowrate of 0.5 mL/min.

The SPR experiments of the binding of the t-CRIS-7 MAB and the B-B12 MAB to SA<sub>v</sub> layers at  $\beta$ CD were performed as follows.  $\beta$ CD SAMs on gold were immersed in a  $10^{-5}$  M aqueous solution of **3** for 15 min, followed by rinsing with Millipore water. Thereafter, the substrate was assembled in the SPR setup. The proteins were flowed over the sample at a concentration of  $1 \times 10^{-7}$  M and at a flow rate of 0.5 mL/min. In between the flows of the different proteins, PBS containing 1 mM  $\beta$ CD was flowed over the substrate.

**Microcontact Printing ( $\mu$ CP).** PDMS stamps were prepared by casting a 10:1 (v/v) mixture of poly(dimethylsiloxane) and curing agent (Sylgard 184, Dow Corning) against a patterned silicon master. After the stamps were cured overnight, they were mildly oxidized in an ozone plasma reactor (Ultra-Violet Products Inc., model PR-100) for 60 min to render them hydrophilic.<sup>49</sup> Subsequently, they were inked by soaking them in a  $10^{-5}$  M aqueous solution of the divalent linker (**3**) for 20 min. The master employed to prepare the PDMS stamps had hexagonally oriented 10  $\mu$ m circular features separated by 5  $\mu$ m. Before printing, the stamps were blown dry in a stream of N<sub>2</sub>. The stamps were applied manually and without pressure control for 10 min onto the  $\beta$ CD monolayers on glass and then carefully removed. For every printing step, a new stamp was used. The substrates were thoroughly rinsed with water. Proteins were flowed over the patterned substrates for 10 min at a flowrate of 0.5 mL/min. In between different protein flows, a rinse of 2 min with PBS was applied.

(48) Ashton, P. R.; Königer, R.; Stoddart, J. F.; Alker, D.; Harding, V. D. *J. Org. Chem.* **1996**, *61*, 903–908.

(49) Bruinink, C. M.; Nijhuis, C. A.; Péter, M.; Dordi, B.; Crespo-Biel, O.; Auletta, T.; Mulder, A.; Schönher, H.; Vancso, G. J.; Huskens, J.; Reinhoudt, D. N. *Chem. Eur. J.* **2005**, *11*, 3988–3996.

**Atomic Force Microscopy.** The AFM experiments were carried out on  $\beta$ CD monolayers on glass. Five substrates were fully covered with **3** by immersion of the substrate in a  $10^{-5}$  M aqueous solution of **3** for 15 min. After that, the samples were rinsed with Millipore water and assembled in a flow cell. The proteins were flowed over the sample at a flow rate of 0.5 mL/min for 10 min. Between protein flows, PBS containing 1 mM  $\beta$ CD was flowed over the substrate.

For the AFM scratching experiments, a custom-built stand-alone AFM was employed.<sup>50</sup> Standard silicon nitride cantilevers with a length of 85  $\mu$ m, force constant 0.5 N/m and operating frequencies 85–130 kHz (in air) purchased from Veeco were used. First, AFM in contact mode was used to produce a 300 nm groove (contact force of 50 nN), by repeatedly scanning the same area to remove the adsorbed material and determine in situ the thickness of the different assemblies. Subsequently, the scan size was increased to 1500 nm and imaged in tapping mode. Images contained  $256 \times 256$  pixels and were recorded at a line frequency of 2 Hz. The calibration of the setup was made with UltraSharp Calibration Gratings from NT-MDT (NT-MDT Co., Russia). Topographical images were quantitatively analyzed by means of Scanning Probe Image Processor program (Image Metrology ApS, Lyngby, Denmark).

**Dot Blot Experiments.** A standard dot blot protocol was used for these experiments.<sup>47</sup> Different concentrations of biotin-CRIS-7, B-B12 in PBS were prepared: 500, 50, and 5 ng/ $\mu$ L. Stock solutions of 1 mg/mL of the enzymes PA-horseradish peroxidase (PA-HRP) and PG-horseradish peroxidase (PG-HRP) were prepared in dilution buffer (PBS). Working dilutions were prepared by diluting the ligand stocks 5000-fold using blocking reagent (containing 0.05% Tween-20 (Surfact-Amps20, product No. 28320, Sigma) and 1% BSA).

Circles ( $d = 4$  mm) were drawn on a Protan nitrocellulose transfer membrane (pore size: 0.45  $\mu$ m, Whatman GmbH, Germany) to indicate the regions in which the protein samples would be blotted. Thereafter, 2  $\mu$ L of the different CD3 MAB solutions were slowly spotted onto the nitrocellulose membrane at the center of the circle using a pipet with a narrow-mouth tip, after which the membrane was left to dry. The nonspecific sites of the membrane (i.e., the sites outside the circled areas) were blocked by soaking the membrane in blocking buffer for 1 h at room temperature. Subsequently, the membranes were removed from the block buffer, and incubated in a solution containing the HRP-conjugate working dilutions for 1 h at room temperature under shaking. After incubation the membranes were rinsed with wash buffer and left shaking in wash buffer. The wash buffer was replaced every 5 min, and this was repeated five times. Thereafter the membranes were incubated in the substrate working solution (a mixture of equal amounts of the stable peroxide solution and the luminol/enhancer solution) for 5 min (0.1 mL of working solution per  $\text{cm}^2$  membrane). Chemiluminescent images of the dot membranes were recorded on a Kodak Image Station 2000MM.

**Lymphocyte Suspensions.** Peripheral blood (20 mL) was collected into 2 heparinized tubes (Venject Lithium Heparin, Terumo, Belgium) from healthy donors. Peripheral blood mononuclear cells (PBMC) were isolated using Ficoll-Paque Plus (GE Healthcare) density separation method. One tube of peripheral blood (approximately 10 mL) was diluted with 12 mL PBS supplemented with 0.38% trisodium citrate (Merck, Germany) and 0.5% bovine serum albumine (Sigma) (PBS-TNC-BSA). A 6–7 mL portion of the diluted blood was brought onto a layer of 3 mL Ficoll with a density of 1.077  $\text{g}/\text{cm}^3$ . The tube was centrifuged at 2200 rpm (1000 g) for 20 min at room temperature. The layer on top of the Ficoll (the mononuclear cells) was removed and washed with about 40 mL PBS-TNC-BSA once at 1500 rpm for 7 min at 4  $^{\circ}\text{C}$ , once at 1400 rpm for 6 min at 4  $^{\circ}\text{C}$ . The mononuclear cells were

resuspended in RPMI 1640 (Gibco, Invitrogen) supplemented with 10% fetal calf serum (FCS, Invitrogen) and 1% antibiotic/antimycotic solution (100 times diluted, Invitrogen), and incubated 1 h at 37  $^{\circ}\text{C}$  in a T75 culture flask. Lymphocytes were concentrated into 2 mL of PBS and kept on ice.

For the cell specificity experiments, a mixture of cells was used, consisting of lymphocytes (90%), which can be subdivided into T-cells, B-cells, and natural killer cells, and monocytes (10%). About 65% of the cells in this mixture are target cells, the ratio between target cells and nontarget cells is therefore about 2:1.

For the linearity experiments, the cell count of the lymphocytes suspension was measured by flow cytometry. Accordingly, four different concentrations of cell suspension were prepared by diluting the original cell suspension with PBS. Four samples were prepared, the cells isolated for the linearity studies were 2016 CD3<sup>+</sup> T cells/ $\mu$ L (sample 1), 1005 CD3<sup>+</sup> T cells/ $\mu$ L (sample 2), 503 CD3<sup>+</sup> T cells/ $\mu$ L (sample 3), and 248 CD3<sup>+</sup> T cells/ $\mu$ L (sample 4).

The lymphocyte solution was put on the AB immobilized glass slides, and left for 30 min in the dark. After that a rinsing procedure was applied in which the cell solution was removed with a pipet. Subsequently, with a new pipet, 200  $\mu$ L PBS was added and removed again. This wash sequence was repeated eight times for an optimal result.

**Cell Enumeration by Immuno-Labeling and Image Recording.**  $\beta$ CD monolayers were prepared on glass substrates which were immersed in a 1 mM aqueous solution of **3**. After rinsing with water, the substrates were mounted in a flow setup, and all protein components were sequentially flowed over the substrate.

For the testing of the different protein–substrates, 200  $\mu$ L of a suspension of lymphocytes ( $1 \times 10^5$  cells/ $\mu$ L), which had been stained with Hoechst 33342 and CD4FITC, was put on top of the substrate, and the cells were incubated for 30 min at room temperature in the dark.

After the cell suspension was removed from the substrate, the substrate was placed under the fluorescence microscope and Hoechst stain images were recorded to determine the optimal washing procedure. The wash procedure consisted of removing the solution from the surface, and replacing it with 200  $\mu$ L of PBS buffer. After eight wash steps the number of cells stained with Hoechst 33342 did not decrease anymore, and images could be recorded.

In the case of the linearity studies, 200  $\mu$ L of a suspension of lymphocytes ( $1 \times 10^5$  cells/ $\mu$ L), was put on top of the substrate, and the cells were incubated for 30 min at room temperature in the dark, followed by the addition of 230  $\mu$ L of a reagent cocktail consisting of 0.5  $\mu$ L of 1 mg/mL Hoechst 33342, 20  $\mu$ L CD3PE, 20  $\mu$ L CD4FITC, 40  $\mu$ L CD8APC, and 150  $\mu$ L of PBS. Four different concentrations of cell suspension were prepared by diluting the original cell suspension with PBS. The solutions for the linearity studies contained 2016 CD3<sup>+</sup> T cells/ $\mu$ L (sample 1), 1005 CD3<sup>+</sup> T cells/ $\mu$ L (sample 2), 503 CD3<sup>+</sup> T cells/ $\mu$ L (sample 3), and 248 CD3<sup>+</sup> T cells/ $\mu$ L (sample 4). The CD3PE cells are sometimes depicted in yellow instead of red, which is caused by an intensity problem.

**Fluorescence Microscopy.** Fluorescent images were made using an Nikon ECLIPSE E400 microscope equipped with a 4  $\times$  objective, four filter cubes (excitation/dichroic/emission: 365/400/400; 480/495/510; 546/560/580; 620/660/700), and a CCD camera for image acquisition.

**Acknowledgment.** We are grateful for financial support from the Council for Chemical Sciences of The Netherlands Organization for Scientific Research (NWO-CW) (M.J.W.L.; Vidi Vernieuwingsimpuls grant 700.52.423 to J.H.).

**Supporting Information Available:** Complete ref 42. This material is available free of charge via the Internet at <http://pubs.acs.org>.

JA078109V

(50) Van der Werf, K. O.; Putman, C. A. J.; De Grooth, B. G.; Segerink, F. B.; Schipper, E. H.; Van Hulst, N. F.; Greve, J. *Rev. Sci. Instrum.* **1993**, *64*, 2892–2897.